Mem. S.A.It. Vol. 74, 379

Memorie della

Nucleosynthesis, the late stages of stellar evolution, chemical and dynamical evolution of late-type galaxies

P. A. Mazzali[1], M. Turatto[2], F. Annibali[3,4], S. Recchi[1], K. Nomoto[5], M. Tosi[4], L. Greggio[2], A. D'Ercole[4], and F. Matteucci[6]

[1] INAF, Osservatorio Astronomico di Trieste, Trieste, Italy
[2] INAF, Osservatorio Astronomico di Padova, Padova, Italy
[3] International School for Advanced Studies, Trieste, Italy
[4] INAF, Osservatorio Astronomico di Bologna, Bologna, Italy
[5] Department of Astronomy, University of Tokyo, Tokyo, Japan
[6] Dipartimento di Astronomia, Università di Trieste, Trieste, Italy

Abstract. Among the topics studied by this program, we have selected here a subset including studies of the energetic core-collapse SNe known as 'Hypernovae', an investigation of the Star Formation History in Late-Type Galaxies and the effect of both the SN explosions and the Star Formation Rate on the chemical and dynamical evolution of Late-Type Galaxies. In particular:
- The recent Type Ic SN 2002ap is spectroscopically a member of the group of Type Ic 'Hypernovae' including SN 1998bw/GRB980425, SN 1997ef, and SN1997dq. Analysis of the spectra and of the light curve of SN 2002ap suggest that it ejected less mass and exploded with a smaller kinetic energy than the other hypernovae, but yet the kinetic energy was significantly larger (4-10 times) than in normal core-collapse SNe. We discuss the implication of the energetics and progenitor mass of 2002ap in the context of the general properties of core-collapse SNe.
- The approach adopted to derive the Star Formation History (SFH) of Late-Type Dwarf Galaxies from the observational Color-Magnitude Diagram is described. We present the results of the SFH inferred in different regions of the Blue Compact Dwarf NGC 1705 through the comparison of synthetic Color-Magnitude Diagrams with HST optical and near infrared photometry. We find that NGC 1705 is not a young galaxy, but has started forming stars at least 5 Gyr ago. While the old population is spread throughout the entire galaxy, the young and intermediate stars are mostly located in the central regions. An interesting result is the presence of a strong burst started only 2 Myr ago and still active.
- The effect of different star formation regimes on the dynamical and chemical evolution of Blue Compact Dwarf galaxies is studied. A 2-D hydrocode, coupled with detailed chemical yields originating from SNeII, SNeIa and from intermediate-mass stars, is used. This type of simulation is applied to a model of galaxy resembling IZw18.

Key words. hydrodynamics – radiative transfer – techniques: spectroscopic – ISM: abundancies – stars:supernovae: general – galaxy: evolution – galaxy: stellar content – gamma rays: bursts

1. The energetics of SN 2002ap in the context of core-collapse SNe

1.1. Introduction

The discovery of a Supernova (SN 1998bw) in the error box of a Gamma-Ray Burst (GRB980425, Galama et al. 1998) was the first evidence of a possible relation between the enigmatic GRB's and a well-studied astrophysical phenomenon.

SN 1998bw was of Type Ic, and so it originated from the explosion of the CO core of a massive star, stripped of its H and He envelopes. However, SN 1998bw was different from previously known SNe Ic: it was a much more energetic event (explosion kinetic energy $E_K \sim 3 \cdot 10^{52}$ erg), as indicated by the very broad absorption lines, which reach velocities of $\sim$ 30000 km s^{-1} (Iwamoto et al. 1998). Because of the broad line features and the high E_K, SN 1998bw was called a 'hypernova'. Also, SN 1998bw ejected a mass of $\sim$ 10 $M_\odot$, much more than typical SNe Ic, indicating a progenitor mass of $\sim$ 40 $M_\odot$. Finally, SN 1998bw synthesized $\sim$ 0.5 $M_\odot$ of radioactive ^{56}Ni, giving rise to a bright, extended light curve.

Further studies revealed that the ejecta of SN 1998bw are probably rather asymmetric (Mazzali et al. 2001), although the degree of this asymmetry is controversial (Höflich et al. 1999; Maeda et al. 2002). Asymmetric models have been able to reproduce some of the observed features, such as the light curve or the late-time spectra. The latter are peculiar, in that the [Fe II] lines are broader than the [O I] 6300Å line (Mazzali et al. 2001). The estimate of E_K is smaller in the asymmetric models ($2 - 10 \cdot 10^{51}$ erg), because the SN was observed near the direction of the jet which probably also caused the GRB.

Although SN 1998bw was certainly an exceptional case, other peculiar SNe Ic were later discovered or recognized. They have in common very broad absorption features, indicative of a high ejecta velocity and hence of a large E_K. Analysis has shown that their properties are not constant, indicating a range of progenitors.

One particularly well studied object is SN 1997ef. Its properties were similar to those of SN 1998bw, although not as extreme. SN 1997ef produced $\sim$ 0.15 $M_\odot$ of ^{56}Ni and ejected $\sim 8\,M_\odot$ of material with $E_K \sim 8 \cdot 10^{51}$ erg (Iwamoto et al. 2000). The progenitor probably had a mass of $\sim 35\,M_\odot$. Further spectroscopic analysis (Mazzali et al. 2000) showed that the observed line widths can only be reproduced if a small amount of matter is moving at $v \sim 30000\,\mathrm{km\,s^{-1}}$, which is not as fast as in SN 1998bw but still makes the E_K estimate increase to $\sim 2 \cdot 10^{52}$ erg. A similar result was obtained also for SN 1998bw (Branch 2001).

In the case of SN 1997ef, there is some evidence that 1D explosion models may not reproduce the observations perfectly. This evidence is derived from the presence of significant line absorption at low velocity ($\sim 2000\,\mathrm{km\,s^{-1}}$). This is well below the supposed cutoff in the ejecta distribution in velocity which results from the formation of a compact remnant (probably a Black Hole for both SNe 1998bw and 1997ef). However, the inconsistent relative width of the Fe and O lines is not seen in the late-time spectra of SN 1997ef, which may suggest that either this event was not very asymmetric or, if it was, that it was not observed near the jet direction. This is consistent with the apparent lack of an associated GRB (a possible correlation is only weak, see Wang & Wheeler 1998).

Other SNe Ic have been observed that are very similar to SN 1997ef. One example is SN 1997dq (Matheson et al. 2001), whose earliest available spectrum looks very similar to those of SN 1997ef at an epoch of 3–4 months. Unfortunately, early observations for SN 1997dq are not available. However, nebular spectra of SN 1997dq are available at epochs when spectra of SN 1997ef are not. This allowed us to estimate that

Send offprint requests to: P. A. Mazzali
Correspondence to: INAF, Osservatorio Astronomico di Trieste, Via Tiepolo 11, I-34131 Trieste, Italy

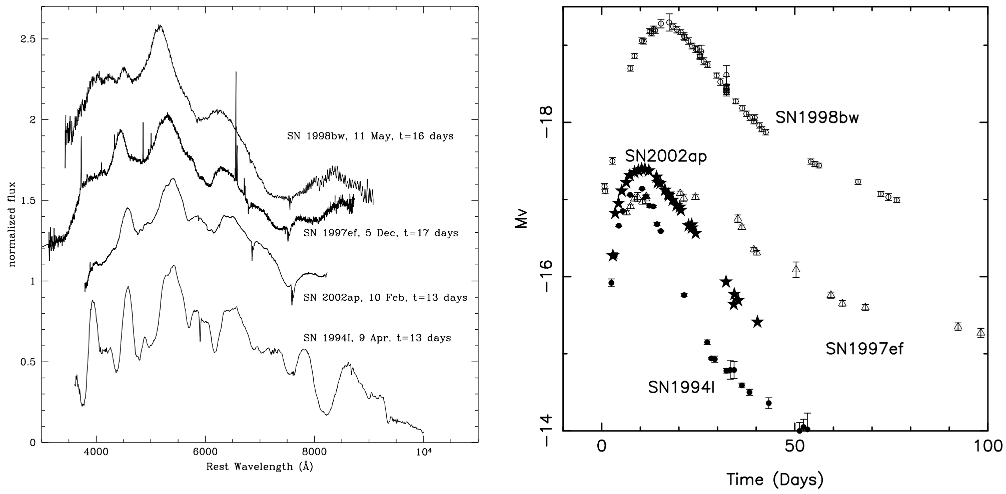

Fig. 1. The near-maximum spectra (left panel) and the absolute V-band light curves (right panel) of Type Ic SNe: SNe 1998bw (squares), 1997ef (triangles), 2002ap (stars), and 1994I (circles) (Mazzali et al. 2002).

the ^{56}Ni mass of both SNe is $\sim 0.17\ M_\odot$ (Mazzali et al. 2002, in preparation). Single spectra of SNe 1999ey (Garnavich et al. 1998) and 2002bl (Armstrong et al. 2002) suggest that these objects are also similar to SN 1997ef. Other very energetic SNe have been discovered among those that interact with the CSM: SNe 1997cy and 1999E (Turatto et al. 2000; Rigon et al. 2003). Both these objects have the intriguing characteristic that they are consistent in position and time with BATSE events.

It appears, as we have discussed, that the properties of these energetic, broad-lined SNe Ic are varied, as confirmed by the latest example of a SN Ic hypernova.

1.2. SN 2002ap

The Type Ic SN 2002ap was discovered in M74 on 2002 January 30 (Hirose 2002). SN 2002ap was immediately recognized as a hypernova from its broad spectral features (Gal-Yam et al. 2002, and references therein) . Luckily, the SN was discovered very soon after it exploded: the discovery date was Jan 29, while the SN was not detected on Jan 25 (Nakano et al. 2002).

Fig. 1a shows the maximum-light spectra of SN 2002ap, of the hypernovae SNe 1998bw and 1997ef, and of the normal SN Ic 1994I, and Fig. 1b shows their V-band light curves. If line width is the distinguishing feature of a hypernova, then clearly SN 2002ap is a hypernova, as its spectrum resembles that of SN 1997ef much more than that of SN 1994I. Line blending in SN 2002ap and SN 1997ef is comparable. However, some individual features that are clearly visible in SN 1994I but completely blended in SN 1997ef can at least be discerned in SN 2002ap (e.g. the Na I–Si II blend near 6000 Å and the Fe II lines near 5000 Å). Therefore, spectroscopically SN 2002ap appears to be located just below SN 1997ef in a 'velocity scale', but far above SN 1994I, as seems to be confirmed by the properties of the light curve. The light curve of SN 2002ap peaks earlier than both hypernovae 1998bw and 1997ef, but later than the normal SN 1994I, suggesting an intermediate value of the ejecta mass $M_{\rm ej}$.

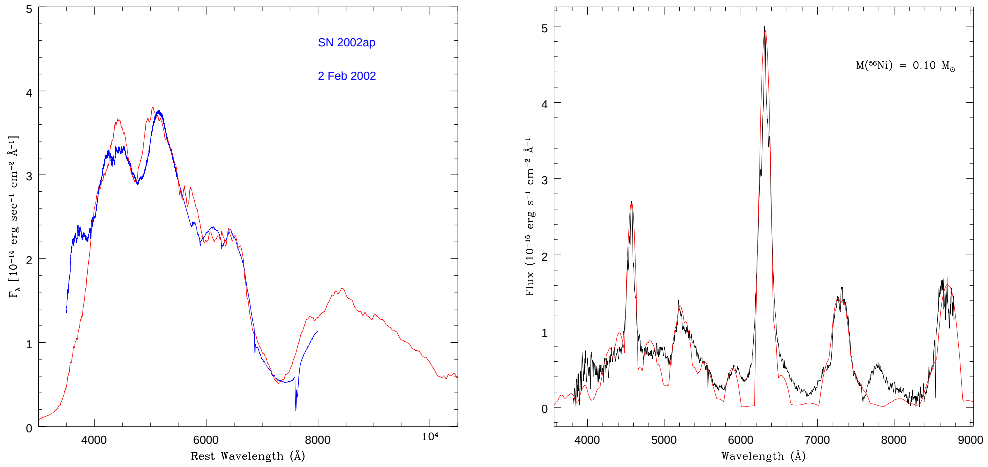

Fig. 2. A spectrum of SN 2002ap observed on Feb. 2, 2002 (left panel), compared to a synthetic spectrum obtained with our Monte Carlo code (Mazzali & Lucy 1993; Mazzali 2000). A spectrum of SN 2002ap observed at Beijing Astronomical Observatory on July 11, 2002 (right panel), compared to a synthetic NLTE spectrum computed for a ^{56}Ni mass of 0.1 $M_\odot$ and a total mass of ≈ 1.3 $M_\odot$ below 6000 km s^{-1}.

Using a distance to M74 of 8 Mpc ($\mu = 29.5$ mag; (Sharina et al. 1996)), and a combined Galaxy/M74 reddening $E(B-V) = 0.09$ mag (Takada-Hidai et al. 2003), the absolute magnitude of SN 2002ap is $M_V = -17.4$. This is comparable to SN 1997ef and fainter than SN 1998bw by almost 2 mag. Since peak brightness depends on the ejected ^{56}Ni mass, SNe 2002ap, 1997ef, and 1994I appear to have synthesized similar amounts of ^{56}Ni. Estimates were $\sim 0.07\,M_\odot$ for SN 1994I (Nomoto et al. 1994) and 0.13 $M_\odot$ for SN 1997ef (Mazzali et al. 2000). The ^{56}Ni mass for SN 2002ap is estimated to be ~ 0.07 $M_\odot$, which is similar to that of normal core-collapse SNe such as SNe 1987A and 1994I.

The spectral evolution of SN 2002ap resembles that of SN 1997ef, at a rate about 1.5 times faster. The model which best reproduces the spectra and the light curve of SN 2002ap has $M_{\rm ej}$= 2.5–5 $M_\odot$ and $E_K = 4-10\cdot10^{51}$ erg (see Fig. 2a). Both $M_{\rm ej}$ and E_K are much smaller than in SNe 1998bw and 1997ef (but they could be larger if a significant amount of He is present).

Although SN 2002ap appears to lie between classical core-collapse SNe and hypernovae, it should be regarded as a hypernova because its kinetic energy is distinctly higher than for classical core-collapse SNe. In other words, the broad spectral features that characterize hypernovae are the results of a high kinetic energy. Also, SN 2002ap was not more luminous than normal core-collapse SNe. Therefore brightness alone should not be used to discriminate hypernovae from normal SNe, while the criterion should be a high kinetic energy, accompanied by broad spectral features. Further examples of hypernovae are necessary in order to establish whether a firm boundary between the two groups exists.

For these values of E_K, $M_{\rm ej}$, and $M(^{56}{\rm Ni})$, we can constrain the progenitor's main-sequence mass $M_{\rm ms}$ and the remnant mass $M_{\rm rem}$. The model which is most consistent with our estimates is one with a C+O core mass $M_{\rm CO} \approx 5\,M_\odot$, $M_{\rm rem} \approx 2.5\,M_\odot$, and $E_K = 4\cdot10^{51}$ erg. Such a core forms in a He core of mass $M_\alpha \approx 7\,M_\odot$, corresponding to $M_{\rm ms} \approx 20-25\,M_\odot$. The non-

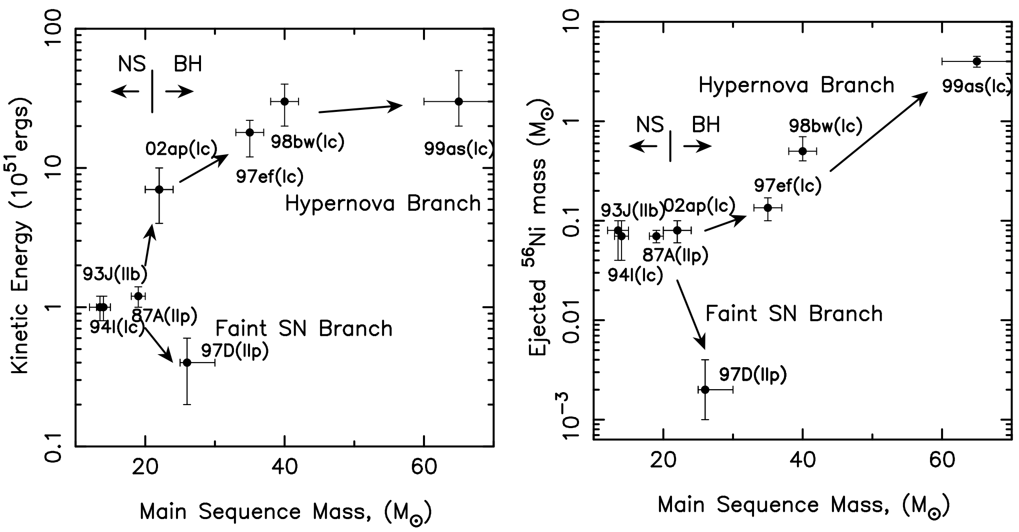

Fig. 3. Explosion energies (left panel) and ejected ^{56}Ni mass (right panel) against main sequence mass of the progenitors for several core collapse supernovae/hypernovae (Nomoto et al. 2002).

detection of the progenitor in pre-discovery images of M74 (Smartt et al. 2002), suggests that the progenitor lost mass through binary interaction. The spiral-in of a companion star is probably required for the progenitor to lose its hydrogen and some (or most) of its helium envelope before collapse (Nomoto et al. 2001). This would suggest that the progenitor was in a state of high rotation. A high rotation rate and/or envelope ejection may also be necessary conditions for the birth of a hypernova.

SN 2002ap was not apparently associated with a GRB. This is actually not so surprising, since the E_K of SN 2002ap is about 5-10 times smaller than that of SN 1998bw, as also indicated by the weak radio signature (Berger et al. 2002). The available data show no clear signature of asymmetry, except perhaps for some polarisation, which is smaller than in SN 1998bw (Kawabata et al. 2002; Leonard et al. 2002; Wang et al. 2002). This suggests that the degree of asphericity is smaller in SN 2002ap and that the possible 'jet' may have been weaker, making GRB generation more difficult. It is also possible that a GRB did occur, but that it was not observed because of an unfavourable inclination with respect to the line-of-sight. Asymmetric models indeed show more 'normal' properties away from the jet axis.

Nebular spectra, which developed at an epoch of about 4 months, do not show the peculiar narrow [O I] 6300Å line as in SN 1998bw, but they do show a narrow core in both [O I] and Mg II 4571Å, which may be interpreted as a signature of asymmetry. The mass of ^{56}Ni estimated from modelling these spectra with a 1D NLTE code (Fig. 2b) is $\approx 0.1\,M_\odot$.

1.3. Energetics in core–collapse SNe

The estimated progenitor mass and explosion energy of SN 2002ap are both smaller than those of previous 'hypernovae' such as SNe 1998bw and 1997ef, but larger than those of normal core-collapse SNe. There appears to be a correlation between $M_{\rm ms}$ and E_K. Fig. 3a shows the relation as obtained from fitting the optical light curves and spectra for various SNe/hypernovae

(Nomoto et al. 2002). Hypernovae appear to lie at the massive end of SN progenitors.

Our analysis suggests that the E_K may also be related to $M_{\rm ms}$. Fig. 3b shows $M(^{56}\rm Ni)$ against $M_{\rm ms}$ (Nomoto et al. 2002). The amount of ^{56}Ni appears to increase with increasing $M_{\rm ms}$ of the progenitor, except for SN II 1997D (Turatto et al. 1998).

Further observational examples are needed to confirm these relations. In particular, it is unclear what fraction of massive stars with $M \gtrsim 20\,\rm M_\odot$ explode energetically. Massive core-collapse SNe with either a normal explosion energy (e.g., SN 1984L; Swartz & Wheeler 1991) or a very small one (SN 1997D; Turatto et al. 1998; Zampieri et al. 2003) also appear to exist.

This trend might be explained as follows. Stars with $M_{\rm ms} \lesssim 25\ \rm M_\odot$ form a neutron star, producing $\sim 0.08 \pm 0.03\ \rm M_\odot$ of ^{56}Ni (e.g. SN IIb 1993J, SN Ic 1994I, and SN 1987A, although SN 1987A may be a borderline case between neutron star and black hole formation). Stars with $M_{\rm ms} \gtrsim 25\,\rm M_\odot$ form a black hole (e.g. Ergma 1998); whether they become hypernovae or faint SNe may depend on the angular momentum in the collapsing core. For SN 1997D, because of the large gravitational potential, the explosion energy was so small that most ^{56}Ni fell back onto a compact remnant; such fall-back might cause the collapse of the neutron star into a black hole. The core of SN II 1997D might not have had a large angular momentum: if the progenitor had a massive H-rich envelope, core angular momentum may have been transported to the envelope possibly via a magnetic field. Hypernovae such as SNe 1998bw, 1997ef, and 2002ap may have had rapidly rotating cores owing possibly to the spiraling-in of a companion star in a binary system. Mass-loss rate and binarity certainly influence the outcome.

The result that the mass of ^{56}Ni synthesized in core-collapse supernovae may be a function of the main-sequence mass of the progenitor star is important for the chemical evolution of galaxies.

2. The Star Formation History in NGC 1705

2.1. Introduction

The evolution of late-type dwarf galaxies and their star formation history has been the subject of numerous studies in the past 10-15 years. This interest is due to the relation between late-type dwarfs and cosmology. Their high gas content and low metallicity make them very similar to primeval galaxies (e.g. Izotov & Thuan 1999) and thus useful tools to get information about primordial galaxy conditions and Big-Bang nucleosynthesis products. In hierarchical models for structure formation, dwarfs are the basic building blocks out of which any other type of galaxy is assembled. Furthermore, Dwarf Irregulars (DIrrs) and Blue Compact Dwarfs (BCDs) have been suggested to be the local counterparts of the faint blue objects in excess in deep galaxy counts at intermediate redshift (e.g. Lilly et al. 1995; Babul & Ferguson 1996). In order to study in details the contribution of these systems to the faint blue galaxy excess, it is of crucial importance to determine both the ages of their stellar populations and the strength of the SF episodes. The most direct estimate of the epochs and of the intensities of the SF activities is derivable from the color-magnitude diagrams (CMDs) of their resolved stellar populations, since the CMD morphology is the direct signature of the star evolutionary conditions.

Here we present the results on the SFH derived for different regions of the BCD NGC 1705 from HST optical (F814W and F555W bands) and near infrared (F110W and F160W bands) photometry (Tosi et al. 2001, hereafter T01). NGC 1705 presents characteristics very similar to the exceptionally active dwarf NGC 1569, and shows the best observational evidence of galactic winds triggered by supernova explosions

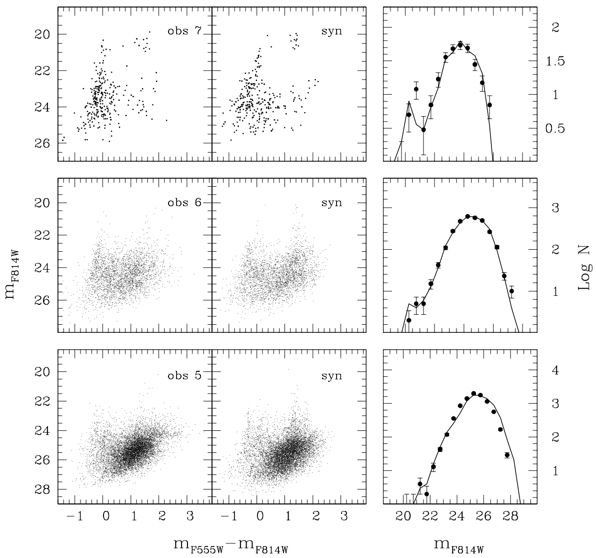

Fig. 4. Comparison between data and models.Top, central and bottom panels correspond respectively to Region 7, 6 and 5. Left to right: the observed CMD, our best synthetic case, the observed (dots) and synthetic (solid line) LFs (see Annibali et al. 2002 for details).

(Meurer et al. 1992; Heckman et al. 2001). Through a spatial analysis of the populations of NGC 1705 we want to map the strengths and ages of the SF episodes over the galaxy area and get then fundamental information about its evolution.

2.2. The method

The SFH can be inferred through the comparison of the observed CMDs with synthetic ones constructed through a Monte Carlo simulation code (Tosi et al. 1991; Greggio et al. 1998) based on homogeneous sets of stellar evolutionary tracks.

The free theoretical parameters are the metallicity, the age, the initial mass function (IMF). The procedure takes into account all the observational uncertainties, i.e. photometric errors, incompleteness, blending of images. The sets of theoretical parameters producing the best agreement between synthetic and observed CMDs (and their corresponding luminosity functions - LFs) are used to constrain the range of possible evolutionary models.

2.3. The application to NGC 1705

We present the SFH inferred with the method of synthetic CMDs only for the three most central regions of NGC 1705 (Region 7, 6 and 5). For a complete derivation of the SFH from Region 7 through 0 (the most external one) see Annibali et al. (2002, submitted).

We have adopted the homogeneous sets of stellar evolutionary tracks computed by the Padova group for various metallicities ($Z = 0.0004$, $Z = 0.004$, $Z = 0.008$, Fagotto et al. 1994a,b). The value of $Z = 0.004$ corresponds to the metallicity derived from H II regions spectroscopy (Storchi-Bergmann, Calzetti & Kinney 1994), while the very metal poor tracks $Z = 0.0004$ were used to account for the first SF episodes possibly occurred in a much metal poorer environment. The adopted distance modulus is $(m - M)_0 = 28.54$ (T01) and $E(B-V) = 0.04$. We have also adopted the incompleteness factors and photometric errors distributions derived with the artificial stars experiments described in T01.

For each region we performed several simulations adopting different starting epochs and SF scenarios (constant and continuous, exponentially decreasing, bursting) and varying the IMF slope (α from 3 to 1.2). In Fig. 4 we present only our best synthetic CMDs. The top, central and bottom sets of panels correspond respectively to Region 7, 6 and 5. In each row, the panels display (left to right) the observed CMD, our best case and the LFs (dots for data, solid line for the best model). It can be noticed how the dropping of the crowding level moving from Region 7 to more external regions allows for the detection of much fainter stars. The observed CMD of Region 7 presents a well-defined blue plume (collecting both main-sequence (MS) stars and the hot edge of the core helium burning phase) and two groups of red objects [one brighter, corresponding to red supergiants (RSGs) with ages between 15 and 10 Myr, and one fainter, due to intermediate mass asymptotic giant branch (AGB) stars]. The best case shown in the second panel has been obtained adopting a burst started 15 Myr ago and stopped 10 Myr ago, with a rate of $\sim 4 \times 10^{-2}$ $M_\odot$ yr^{-1} for a Salpeter's IMF ($\alpha = 2.35$), and a younger stronger episode started only 2 Myr ago and still ongoing at the rate of $\sim 2.7 \times 10^{-1}$ $M_\odot$ yr^{-1}. To reproduce the gap observed between the clump of RSGs and the fainter AGB stars it is necessary to assume that there was no SF between 60 and 15 Myr ago. The high crowding level of Region 7 prevents us to probe ages older than ~ 0.6 Gyr, this limit corresponding to the less massive AGB stars sampled. In Region 6, the dramatic drop of the crowding level with respect to the center allows for the detection of much fainter objects. At $m_{F814W} > 23$ the CMD is populated by stars in the blue loop and

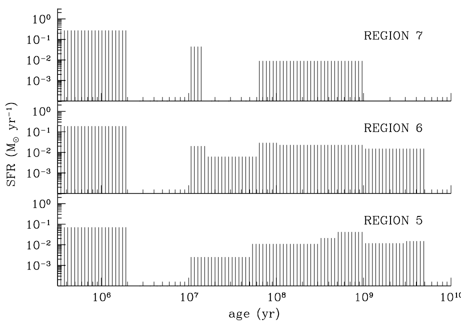

Fig. 5. The derived SFR (for a Salpeter's IMF) versus age for Region 7, 6 and 5 (see Annibali et al. 2002 for details).

AGB phase, while the concentration of objects with $1 < m_{F555W} - m_{F814W} < 1.8$ and $24.2 \leq m_{F814W} \leq 26$, better delineated in Region 5, corresponds to low mass old stars in the red giant branch (RGB) evolutionary phase. The best synthetic case presented in the second panel of the second row of Fig. 4 assumes, as in Region 7, the presence of two bursts (15-10) Myr and (2-0) Myr. Back to 1 Gyr ago the SF derived does not show big gaps between the episodes. Rather than constant, the SF was more likely fluctuating.

We have also assumed a SF activity as old as 5 Gyr ago, accounting for few RGB stars. In the observed CMD of Region 5 (first panel in the bottom) the blue and the red plume are still visible, but they are not so well defined as in Region 6 and 7. Here the crowding level is low enough to allow for the detection of many faint, low mass stars in the RGB phase. Besides, at m_{F814W} just fainter than 24, it is possible to recognize a horizontal feature extending redward of $m_{F555W} - m_{F814W} \sim 2$: we tend to ascribe it to thermally pulsing AGB stars, a poorly understood evolutionary phase whose models are not included in the adopted tracks. Next to the observed CMD we show one of our best models. We still need a very young episode of SF started ~ 2 Myr ago to account for the observed MS stars. Again, at intermediate ages the SF presents some fluctuations in the rate, and long quiescent periods between the SF episodes must be excluded. An activity as old as a few Gyr (5 in the particular case shown) must be assumed to account for the observed RGB phase.

All the best cases presented here assume an IMF like Salpter's or slightly steeper. We tend to exclude a flat IMF. The SFH derived for the three regions is summarized in Fig. 5, where we plot the SFR (obtained under the assumption of a single IMF slope in the mass range 0.1-120 $M_{\odot}$) versus age.

2.4. Conclusions

Our major results are in brief:

- The occurrence of a burst from 15 to 10 Myr ago (i.e. with the same age of the central super star cluster), mostly occurred in the central regions of NGC 1705.
- A much younger burst (from $\sim$ 2 Myr ago to now), occurred with a very strong intensity in the central regions but present also, at a lower rate, in more external regions (see Annibali et al. 2002).
- The presence of a population at least 5 Gyr old, probably (we cannot probe such old ages in the center) spread throughout the entire galaxy. Instead, the young and intermediate stars are mostly located in the central regions.

3. Chemical and dynamical evolution of late-type galaxies

3.1. Introduction

The study of the impact of Supernova explosions and stellar winds on the evolution of Starburst and Blue Compact Dwarf (BCD) galaxies has been analyzed by means of hydrodynamical simulations by several authors in the recent past. The overall picture is that these galactic winds are not able to eject a significant fraction of the ambient Interstellar Medium (ISM) of the host galaxies after a single burst of star formation, whereas a large fraction of metal-enriched gas produced by the starburst can escape the galaxy potential well (see e.g. MacLow & Ferrara 1999; D'Ercole et al. 1999).

Recent HST observations were deep enough to resolve faint stars in external galaxies and actually in most of BCDs an older stellar population has been observed. A model with a single, instantaneous burst of star formation is thus unfit to describe BCDs. A better approximation is a model with multiple, instantaneous bursts of star formation. Of course, the idea that the star formation in this kind of galaxies is instantaneous is too restrictive. Many authors believe that even BCDs can have a gasping star formation, with long episodes of activity separated by short quiescent intervals. In this work we present a 2-D chemo-dynamical model able to follow in a self-consistent way the chemical and dynamical evolution of BCD galaxies as a consequence of two bursts of star formation, separated by a quiescent period and under a continuous star formation regime.

3.2. The model

With a metallicity of 1/50 $Z_{\odot}$, IZw18 is the most metal-poor galaxy locally known. Recent studies of CMDs both in the optical (Aloisi et al. 1999; hereafter ATG) and in the infrared revealed the presence of two stellar populations: the younger one with an age of 10-15 Myr and an AGB population with an age of several 10^8 years. ATG suggested that the star formation in IZw18 has started at least 300 Myr ago. They suggested a first burst of star formation with a constant star formation rate of $6\cdot 10^{-3}$ $M_{\odot}$ yr^{-1} in the first 270 Myr. This first episode of star formation is followed by a short quiescent period of 10 Myr. A second, stronger burst of star formation has occurred recently, from 20 to 15 Myr ago, with a SFR of $3\cdot 10^{-2}$ $M_{\odot}$ yr^{-1}.

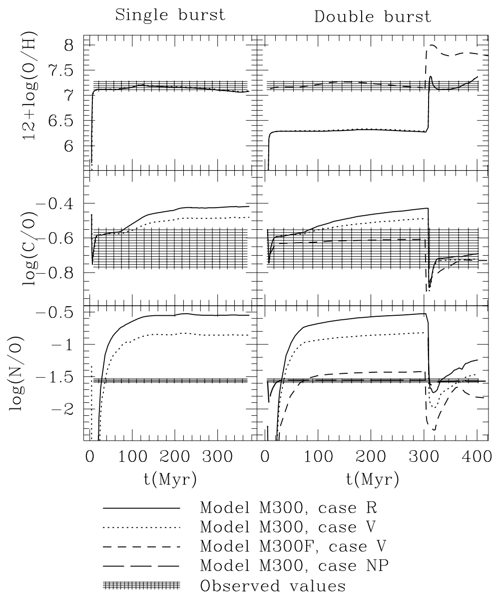

Fig. 6. Evolution of O, C, N for the single-burst model (left panels) and models M300 and M300F (right panels). In the bottom-right panel we show the evolution of N/O for a model (model NP) in which we assumed an 'ad hoc' production of primary N in massive stars. The superimposed dashed areas represent the observative values found in literature for IZw18.

3.2.1. Instantaneous double-burst model

As a first approach, we considered two instantaneous bursts. The initial conditions of the model are the same adopted in (Recchi et al. 2001, hereafter R01), namely a rotating gaseous component in hydrostatic isothermal equilibrium with a galactic potential well and the centrifugal force. The thermal energy is provided by SNe and stellar winds. According to R01, we choose a low thermalization efficiency for SNeII and a larger value (100%) for SNeIa, since this kind of objects explode in a medium already heated and diluted by the previous activity of SNeII.

According to the star formation history inferred by ATG, we assume a first burst of star formation occurring 300 Myr ago and producing 10^5 $M_\odot$ of stars, distributed according to a Salpeter IMF (model M300). A model with a flatter (x = 0.5) IMF, as suggested by ATG, is also considered (M300F). The initial metallicity of the gas is set to zero. Owing to the low luminosity of this first burst, galactic winds do not form. After 300 Myr most of the mass in the central region (a sphere of 200 pc of radius) is cold and dense, thus the onset of a second burst of star formation is likely. The assumed metallicity for this second burst is 1/50 of solar value, namely the metallicity of the cold gas in the central region at the onset of the burst.

Owing to the thermodynamical conditions of the central region, the impact of the energetic input of the second generation of stars on the ISM dynamics is rather strong. A breakout occurs already after 30 Myr and the gas produced by the second generation of stars is easily channelled along the galactic chimney. An even stronger impact is produced by model M300F, since the number of SNeII is 3 times larger than in the standard model. In Fig. 1 we show the evolution of C, N, O for models M300 and M300F, with different chemical prescriptions. Dashed areas represent the observed values found in literature. Also shown is a model with primary N production from massive stars. Assuming an *ad hoc* production of primary N (1/1000 of the initial mass for the whole range of massive stars), we are able to reproduce the observed value of N/O. We fit the abundances observed in IZw18 under the assumption that the last starburst has an age between 4 and 6 Myr, depending on the model and in agreement with the Spectral Energy Distribution.

3.2.2. Continuous burst model

We adopt the star formation law suggested by ATG. We calculate the mass of stars formed between t and t + Δt, where Δt $\sim$ 10^5 yr. This *Stellar Population* (SP) is treated as a starburst. We thus assume a Salpeter IMF and calculate the mass, energy and metal released by each SP. The

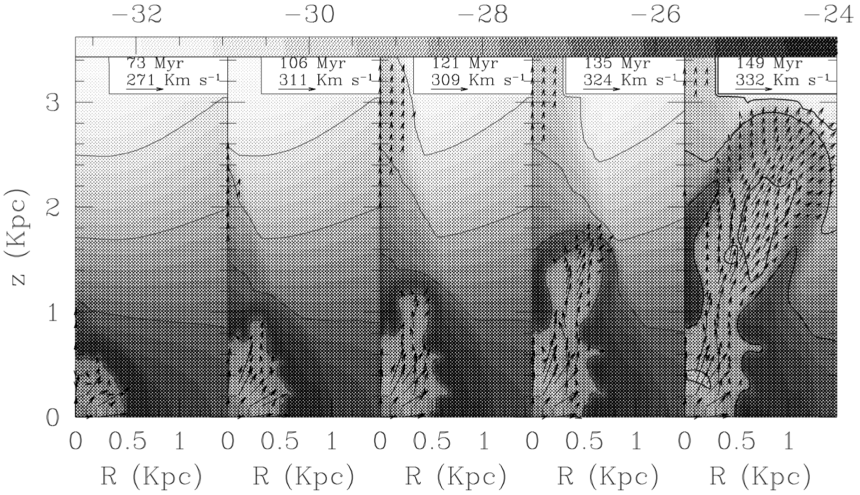

Fig. 7. Density contours and velocity field for a model with a continuous SF. Evolutionary times are labelled in a box on top of each panel.

metals released by each SP can be calculated according to their metallicity. The input rate from SNeII, SNeIa and single, intermediate-mass stars for each chemical element l is calculated summing all the contributions from each SP. We consider both the contribution of newly synthesized metals ($P_l(m)$), and of metals released by the stars but unmodified by nucleosynthetic processes. The latter contribution depends on the metallicity of the SP. We assume for the moment a SF occurring at the center of the system and a constant metallicity of $1/100\ Z_{\odot}$.

The continuous burst model predicts a galactic wind occurring before the onset of the second burst. The metallicity observed in IZw18 is reproduced between ~ 5 and 15 Myr after the onset of the second burst. The age of the more recent burst in IZw18 should be thus in this range (5-15 Myr). However, at this time, 25% of the ambient ISM is lost owing to the wind. A snapshot of the evolution of this model is shown in Fig. 2.

Acknowledgements. This work was supported in part by the Italian Ministry for Education, University and Research (MIUR) through grants Cofin 9802909231 and MM02905817.

References

Aloisi, A., Tosi, M., & Greggio, L. 1999, AJ, 118, 302 (ATG)
Armstrong, M., et al. 2002, IAU Circ., 7845
Babul, A., & Ferguson, H. C. 1996, ApJ, 458, 100
Berger, E., Kulkarni, S. R., & Frail, D. A. 2002, IAU Circ., 7817
Branch, D. 2001, in Supernovae and Gamma-Ray Bursts, ed. M. Livio, N. Panagia, & K. Sahu (Cambridge: CUP), 96
D'Ercole, A., & Brighenti, F. 1999, MNRAS, 309, 941
Ergma, E., & van den Heuvel, E. P. J. 1998, A&A, 331, L29
Fagotto, F., Bressan, A., Bertelli, G., & Chiosi, C. 1994a, A&AS, 105, 29
Fagotto, F., Bressan, A., Bertelli, G., & Chiosi, C. 1994b, A&AS, 104, 365

Galama, T. et al. 1998, Nature, 395, 670
Gal-Yam, A., Ofek, E. O., & Shemmer O. 2002, MNRAS, 332, L73
Garnavich, P., Jha, S., & Kirshner, R. 1998, IAU Circ., 7066
Greggio, L., Tosi, M., Clampin, M., de Marchi, G., Leitherer, C., Nota, A., & Sirianni, M. 1998, ApJ, 504, 725
Hirose, Y. 2002, IAU Circ., 7810
Höflich, P., Wheeler, J. C., & Wang, L. 1999, ApJ, 521, 179
Iwamoto, K., Mazzali, P. A., et al. 1998, Nature, 395, 672
Iwamoto, K., et al. 2000, ApJ, 534, 660
Izotov, Y. I., & Thuan, T. X. 1999, ApJ, 511, 639
Heckman, T. M., Sembach, K. R., Meurer, G. R., Strickland, D. K., Martin, C. L., Calzetti, D., & Leitherer, C. 2001, ApJ, 554, 1021
Kawabata, K. S., Jeffery, D., Kosugi, G., Sasaki, T., et al. 2002, ApJ, submitted (astro-ph/0205414)
Leonard, D., Filippenko, A. V., Chornock, R., & Foley, R. 2002, PASP, 114, 1133
Lilly, S. J., Tresse, L., Hammer, F., Crampton, D., & Le Fevre, O. 1995, ApJ, 455, 108
MacLow, M.-M., & Ferrara, A. 1999, ApJ, 513, 142
Maeda, K., Nakamura, T., Nomoto, K., Mazzali, P. A., Patat, F. & Hachisu, I. 2002, ApJ, 565, 405
Matheson, T., Filippenko, A. V., Li, W., Leonard, D. C., & Shields, J. C. 2001, AJ, 121, 1648
Mazzali, P. A. 2000, A&A, 363, 705
Mazzali, P. A., & Lucy, L. B. 1993, A&A, 279, 447
Mazzali, P. A., Iwamoto, K., & Nomoto, K. 2000, ApJ, 545, 407
Mazzali, P. A., Nomoto, K., Patat, F., & Maeda, K. 2001, ApJ, 559, 1047
Mazzali, P. A., et al. 2002, ApJ, 572, L61
Meurer, G. R., Freeman, K. C., Dopita, M. A., & Cacciari, C. 1992, AJ, 103, 60
Nakano, S., Kushida, R., & Li, W. 2002, IAU Circ., 7810
Nomoto, K. et al. 1994, Nature, 371, 227
Nomoto, K. et al. 2001, in Supernovae and Gamma-Ray Bursts, ed. M. Livio, N. Panagia, & K. Sahu (Cambridge: CUP), 144
Nomoto, K. et al. 2002, IAU Symposium 212, A massive Star Odyssey, from Main Sequence to Supernova, ed. V. D. Hucht, A. Herrero, & C. Esteban (San Francisco: ASP), ASP Conf. Ser., in press (astro-ph/0209064)
Recchi, S., Matteucci, F., & D'Ercole, A. 2001, MNRAS, 322, 800 (R01)
Rigon, L., et al. 2003, MNRAS, in press
Sharina, M. E., Karachentsev, I. D., & Tikhonov, N. A. 1996, A&AS, 119, 499
Smartt, S. J., Vreeswijk, P., Ramirez-Ruiz, E., et al. 2002, ApJ, 572, L147
Storchi-Bergmann, T., Calzetti, D., & Kinney, A. L. 1994, ApJ, 429, 572
Swartz, D. A., & Wheeler, J. C. 1991, ApJ, 379, L13
Takada-Hidai, M., Aoki, W., & Zhao, G. 2003, PASJ, submitted
Tosi, M., Greggio, L., Marconi, G., & Focardi, P. 1991, AJ, 102, 951
Tosi, M., Sabbi, E., Bellazzini, M., Aloisi, A., Greggio, L., Leitherer, C., & Montegriffo, P. 2001, AJ, 122, 1271
Turatto, M., Mazzali, P. A., et al. 1998, ApJ, 498, L129
Turatto, M., Suzuki, T., Mazzali, P. A., et al. 2000, ApJ, 534, L57
Wang, L., & Wheeler, J. C. 1998, ApJ, 504, L87
Wang, L., Baade, D., Höflich, P., Wheeler, J. C., et al. 2002, ApJ, submitted (astro-ph/0206386)
Zampieri, L., Pastorello, A., Turatto, M., Cappellaro, E., Benetti, S., Altavilla, G., Mazzali, P., & Hamuy, M. 2003, MNRAS, in press